



Catalytic oxidation of Methyl Orange by an amorphous FeOOH catalyst developed from a high iron-containing fly ash

Yi Li, Fu-Shen Zhang*

Research Center for Eco-Environmental Sciences, Chinese Academy of Sciences, 18 Shuangqing Road, Beijing 100085, China

ARTICLE INFO

Article history:

Received 11 August 2009

Received in revised form 7 December 2009

Accepted 12 December 2009

Keywords:

Photo-Fenton

Fly ash

UV/H₂O₂

Mesoporous structure

Amorphous FeOOH

ABSTRACT

Heterogeneous photo-Fenton process using an amorphous FeOOH as catalyst was studied to degrade Methyl Orange (MO) dye in aqueous solution. The amorphous FeOOH was prepared by dissolution and precipitation using a high iron-containing fly ash as raw material. The ash not only provided iron source but also acted as a supporter of amorphous FeOOH. Coating the fly ash particles with the amorphous FeOOH significantly enhanced the removal of MO, and 2.5 g of catalyst was sufficient to degrade 50 mg MO from 1 l of aqueous solution at pH 7.0 after 80 min. Oxidant concentration, solution pH, UV/dark/sunlight and recycling of the catalyst were investigated in order to evaluate the photo-Fenton effects. Moreover, variations of particle size before and after preparation, separation of solid–liquid and stability of the amorphous FeOOH in the catalyst were studied. It was testified that the amorphous FeOOH on the surface of fly ash was stable and the Fenton catalyst was easily separated from the aqueous system.

© 2009 Elsevier B.V. All rights reserved.

1. Introduction

The Fenton reaction has its own unique advantage in the degradation of pollutants as one of advanced oxidation processes (AOPs) because its reagents are environmentally benign, cheap and relatively easy to obtain and handle. The traditional homogeneous Fenton reaction works only in the pH range of 2.0–4.0 and tends to be highest at around pH 3.0 and then decreased with increasing pH, for example, the Fenton process nearly comes to halt as the pH increases from 3.0 to 7.0 when *p*-hydroxybenzoic acid was degraded in the system of homogenous Fenton [1]. For overcoming the above disadvantages of the homogeneous Fenton process, the heterogeneous Fenton reaction with aid of light irradiation was developed.

According to previous studies, some crystalline iron hydroxides/oxides (α -FeOOH, γ -FeOOH and γ -Fe₂O₃) [2–5] and supported iron compounds [6–10] as photo-Fenton catalysts have been intensively studied and are thought to be promising effective catalysts in the heterogeneous system. Briefly, their effectiveness is attributed to the production of surface iron complex (e.g. surface Fe (IV) species) and hydroxyl radicals (HO•) when UV irradiation of the surface broke chemical bond. Then the highly oxidized and unstable surface iron complex reacts with water to form a further HO• [2]. Thus, the catalyst experiences an iron cycling on the surface without significant diffusion into the solution phase.

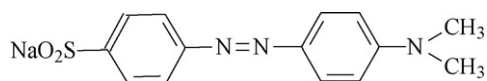
The free hydroxyl radicals are powerful, non-selective oxidants with the ability of decomposing almost all organic contaminants into carbon dioxide and water in aqueous solution, including dyes [8–10].

To our knowledge, however, amorphous FeOOH used as photo-Fenton reagent has not been attempted to degrade pollutants although its surface area is higher than the crystalline iron hydroxides. That is because the amorphous FeOOH is merely available as fine powder or exists as gel or suspension in the solution, hence it is difficult to be separated entirely from the solution. Another shortage of amorphous FeOOH is that it tends to form crystalline iron oxides in the preparation process, which may greatly reduce its degradation capacity since its surface area is greatly diminished, thus a stable and easily separated amorphous FeOOH photo-Fenton catalyst is desired.

The aim of this study was to investigate an amorphous FeOOH photo-Fenton reagent prepared by a high iron-containing fly ash (HICFA). The iron oxide content in this fly ash was as high as 17.52% and the amorphous FeOOH supported on the fly ash particles was prepared by the rearrangement of iron oxide contained in the fly ash.

Wastewater released from textile, painting, leather, printing and photography industries contains some recalcitrant pollutants, especially synthetic dyes, and the presence of small amounts of dyes (below 1 ppm) is clearly visible, and greatly influences the water environment [11]. Besides the aesthetic problem, dyes in wastewater limit the possible use of water and reduce the efficacy of the microbial wastewater treatment because they may be toxic to microorganisms. In this study, Methyl Orange (MO, Scheme 1) dye was selected as a model hydrocarbon due to its environmen-

* Corresponding author. Tel.: +86 10 62849515; fax: +86 10 62849515.
E-mail address: fszhang@rcees.ac.cn (F.-S. Zhang).



Scheme 1. Molecular structure of MO.

tal significance, ease of analysis, and relative solubility in water. The effects of important variables on the degradation of MO were investigated. This study was more concerned about the operational performance of the amorphous FeOOH photo-Fenton reagent for treating the wastewater, so the solid–liquid separation, variations of particle size before and after preparation, stability of amorphous FeOOH and recycling efficiency were investigated in detail.

2. Experimental details

2.1. Materials

Fly ash, a byproduct from power station, is one of the industry solid wastes in China, and the high iron-containing fly ash in this study was sampled from Gaobeidian thermal power plant (4 MW \times 200 MW) located in Beijing (China). The ash was collected by an electrostatic precipitator after the pulverized coal burnt in the cyclone furnace boiler. The fly ash contains element oxides such as SiO₂ 29.33%, Al₂O₃ 25.70%, Fe₂O₃ 17.52%, CaO 22.17%, MgO 1.60%, SO₃ 4.15%, K₂O 0.56%, Na₂O 1.81% and its Loss on Ignition (LOI) is 0.27%.

MO, H₂O₂ (30%), FeCl₃ (AR) and diethyl ether (AR) were purchased from Beijing chemical works. Stocking solution containing 1000 mg l⁻¹ of MO was directly dissolved from pure MO, and MO working solutions were freshly made by diluting stocking solution with distilled water. HCl (1 M, 0.1 M), and NaOH (1 M, 0.1 M) solutions were prepared for pH adjustment.

2.2. Preparation of photo-Fenton catalyst and analysis methods

The photo-Fenton catalyst was prepared by dissolution and precipitation using the high iron-containing fly ash as the raw material. The element Fe in the fly ash was dissolved into the acidic solution, then precipitated as the amorphous FeOOH and simultaneously deposited on the surface of the residual ash particles. The detailed depiction of synthesis process was presented in a previous report [12]. Briefly, the catalyst powder was prepared according to the following procedure: firstly, 3.0 g of the raw fly ash was added into 250 ml of water, and the mixture was stirred and heated to 95 °C for 1 h to remove some alkali and alkaline earth elements in the fly ash, then the insoluble material was filtrated and dried at 100 °C for 2 h. Secondly the pretreated fly ash was contacted with 100 ml of 1 M HCl solution, vibrated (200 r/min) in a rotary shaker (THZ-100, Nanjing chemical apparatus Inc, China) for 2 h and placed steadily at 60 °C for 0.5 h. Thirdly, 1 M NaOH solution was added dropwise into the solution until the final pH was adjusted to about 6.0 (except where otherwise specified). The mixture continuously vibrated for 1 h and aged at 75 °C for 3 days (except where otherwise specified). Finally, the slurry was dewatered by centrifugation and then dried at 75 °C for 24 h. Upon cooling, the composite solid was broken to separate the powders in the carnelian mortar, and afterwards stored in the capped polyethylene bottle for use.

The X-ray diffraction (XRD) patterns of the catalyst were obtained using X-ray diffractometer (Philips PW 1700, Holand) to examine the change of crystalline phase and the operating conditions were 45 kV and 250 mA, using Cu K α radioactive source. The surface morphology was obtained using scanning electron micrograph (SEM) (Hitachi S-3000N, Japan). The technology of laser particle size (LPS) was used to analyze the particle size distribution of raw fly ash and the catalyst by laser particle sizer (Master size

2000, Malvern Co, UK). The BET (Brunauer–Emmet–Teller) specific surface area was determined by fitting the linear portion of the BET plot to BET equation, and average pore size was calculated based on the desorption plot of N₂ adsorption–desorption isotherm using the Barrett–Joyner–Halenda (BJH) method (Micromeritics ASAP 2000, USA). The absorbance of MO solution was examined by the UV–vis spectroscopy (UV-2450, Shimadzu, Japan). The iron leaching iron concentration was examined by inductively coupled plasma optical emission spectrometer (ICP–OES) (PerkinElmer OPTIMA 2000, USA).

2.3. Experimental procedure of photo-Fenton degradation of MO

The UV degradation experiments were carried out inside a 600 m \times 550 mm \times 450 mm stainless box with a door in one side for operating. A UV lamp (GY-250, TIANMEI light source of Beijing, China) with the main emission of 365 nm positioned in the center of reactor was used as an irradiation source, and a series of 100-ml quartz flasks were employed as photo-Fenton reaction vessels. About 21 cm² of surface area in the flasks was directly exposed to the irradiation light, and the photo flux near the flasks was about 60 W m⁻² (UVA radiation meter, photoelectric instrument factory of Beijing Normal University, China). The flasks were stirred magnetically during irradiation. In the experiments, the effects of solution pH (from 5.0 to 7.0), contact time (from 120 to 180 min), irradiation light (sunlight, darkness, UV) and H₂O₂ concentration (0, 5.26, 15.8 and 26.3 mM) were examined so as to optimize operation conditions. The solution was sampled and taken out from the reactor at desired time intervals, and then centrifuged to separate solid from the solution. For avoiding any possible effect of further reaction caused by the HO \cdot after centrifugation, the supernatant was analyzed immediately by UV–vis spectroscopy to test the degradation of MO.

The wavelength of 460.5 nm, which is the maximum absorbance wavelength registered experimentally and is ascribed to the azo bond ($-N \equiv N-$) of the Methyl Orange molecule, was used for evaluation of the MO photodegradation. The photocatalytic degradation conversion was calculated with the following formula without concerning the degradation intermediates,

$$\eta_D = \frac{Abs_0 - Abs_t}{Abs_0} \times 100\% \quad (3)$$

where η_D is the degradation ratio of MO, Abs_0 and Abs_t are the absorbency of MO solution at initial time and after irradiated in t time at 460.5 nm, respectively. Moreover, the experimental data are fitted by applying a pseudo-first-order model $\ln(Abs_t/Abs_0) = -kt$ to determine an observed rate constant (k) of MO in the experiments.

In addition, the solar induced oxidation of MO was performed at Research Center for Eco-Environmental Sciences (RCEES) parking lot (39°48'N; 116°28'E), Chinese Academy of Science (CAS) in Beijing, China. The environmental temperature in the experimental time was 15–18 °C, and the reaction temperature was controlled at 25 °C. The solar irradiation intensity was in range of 540–600 W m⁻² with an average UV irradiation intensity 6 W m⁻². Darkness was realized by wrapping the flask using aluminum foils.

3. Results and discussion

3.1. Characterization of the catalyst

The SEM image of the catalyst is shown in Fig. 1. The amorphous FeOOH loaded on the sphere was irregular porous structure, and the size of catalyst mainly ranged from 15 to 30 μ m. The inner sphere in the catalyst was the residual fly ash after acidized by HCl solution and then coated by the amorphous FeOOH when iron precipitated from solution. So the high iron-containing fly ash not

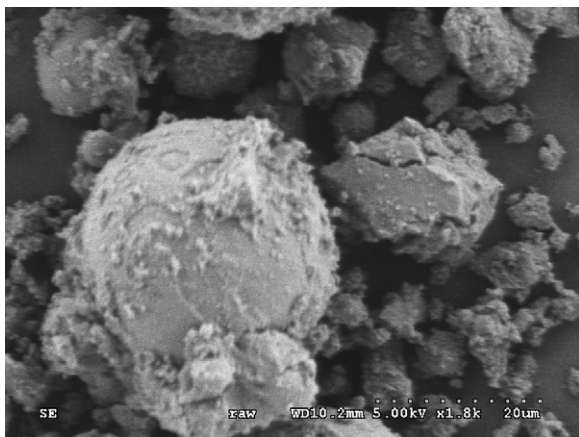


Fig. 1. SEM image of the amorphous FeOOH supported on the fly ash.

only provided iron source in the synthesis process but also worked as the supporter of amorphous FeOOH. Moreover, no crystalline FeOOH was found in the image of XRD. The average pore size of catalyst is 23 Å and its BET specific surface area is 140 m²/g. More detailed properties of IR, XRD, porosity, pore distribution and the other information were shown elsewhere [12].

3.2. Effects of the photo-Fenton experiments

Due to the dissolution of the solid catalyst in acidic water to produce ferrous ions in heterogeneous system, the catalyst will inevitably increase the catalytic efficiency of MO when the pH was adjusted to below 3.0 [13], moreover Chou et al. [4] also reported that the homogeneous catalysis was insignificant at pH > 4.4 when oxidizing Benzoic acid using γ -FeOOH catalyst because the dissolved iron concentrations were very low. For enhancing catalysis, UV light was introduced into the heterogeneous Fenton system at a higher pH. In our study, in order to evaluate the contribution of UV light to the heterogeneous Fenton when the solution is neutral or alkaline, the solar and dark Fenton were also studied.

The MO concentration hardly declined with only UV irradiation in the absence of H₂O₂ or catalyst, indicating that the degradation of MO by photolysis was very weak and negligible. Fig. 2(a) shows the changes of MO under the conditions of darkness, solar and ultraviolet irradiation with H₂O₂ at initial pH 7.0. Both removals of MO in the system by darkness and sunlight irradiation within 120 min fluctuated from 6.0 to 11.0% which were attributed to the adsorption of the catalyst and possible homogeneous process, and the fluctuation of removal would be ascribed the unbalanced adsorption–desorption between the MO molecule and the catalyst. Meanwhile it indicates that the sunlight was not enough to promote the catalytic process when the solution is neutral, which was not as effective as Fenton reaction in the acidic solution [14]. On the other hand, 2.5 g of catalyst was sufficient to degrade 50 mg of MO from 1 l of aqueous solution after 80 min UV irradiation. The high degradation should be ascribed to the utilization of UV light with the high irradiation intensity, moreover after the catalytic process was initiated by the UV light, the combined effect of adsorption [12] and high interface area of the catalyst could also enhance the Fenton process.

The influence of oxidant concentration on the heterogeneous photo-Fenton degradation of MO by the amorphous FeOOH was tested by adding different concentrations of hydrogen peroxide (0, 5.26, 15.8 and 26.3 mM). Fig. 2(b) shows that the equilibrium removal ratio was about 6% after 120 min without addition of hydro peroxide, which was attributed to the adsorption of the catalyst. Nevertheless, when 5.26, 15.8 and 26.3 mM H₂O₂ were added into

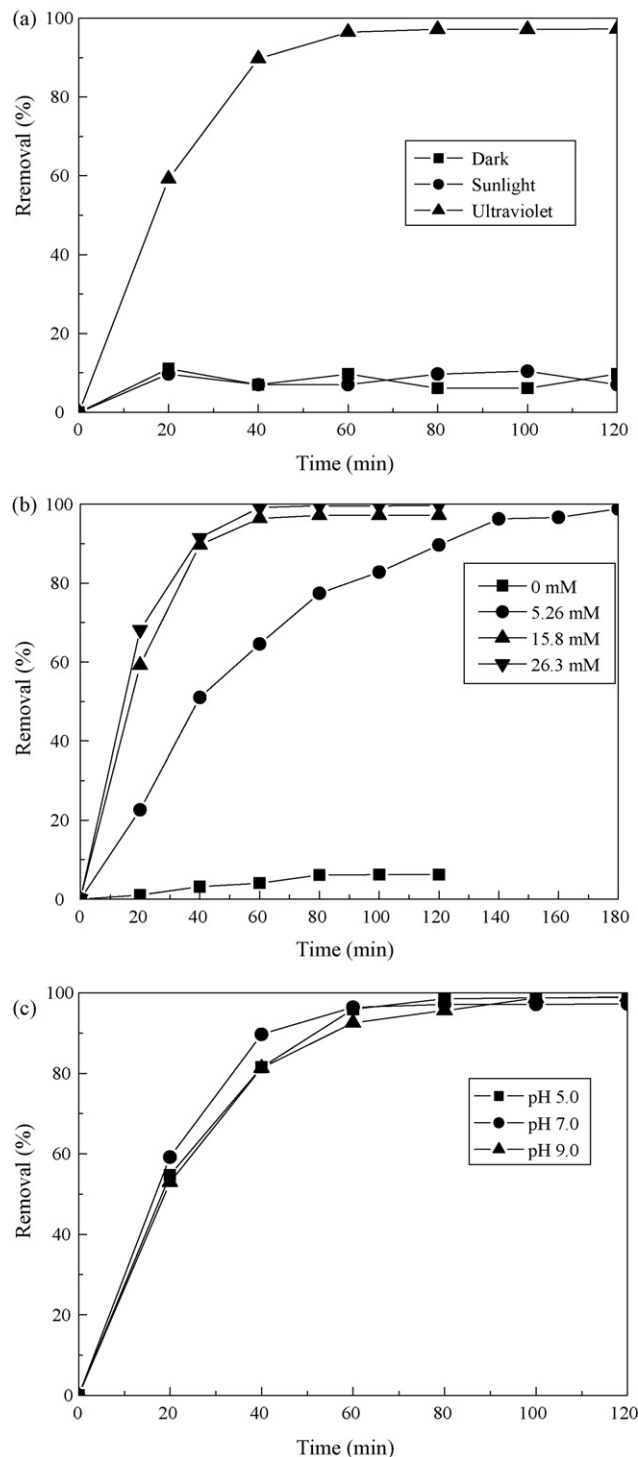


Fig. 2. Degradation of MO as a function of (a) light, (b) H₂O₂ and (c) pH. Experimental conditions for (a): MO concentration = 50 mg l⁻¹, catalyst dose = 2.5 g l⁻¹, H₂O₂ concentration = 15.8 mM, pH 7.0; for (b): MO concentration = 50 mg l⁻¹, catalyst dose = 2.5 g l⁻¹, pH 7.0, light irradiation = UV; for (c) MO concentration = 50 mg l⁻¹, catalyst dose = 2.5 g l⁻¹, H₂O₂ concentration = 15.8 mM, and light irradiation = UV.

the solution as oxidants, the photodegradations of MO after 20 min irradiation enhanced to 22.6%, 59.2% and 68.0%, respectively, which indicated an increase of MO conversion with increasing oxidant concentrations. After 60 min irradiation, the solution of MO in the higher oxidant concentration (15.8 and 26.3 mM) was decolorized fully, while that in low concentration (5.26 mM) attained only 64.5%. On the other hand, when extending irradiation time

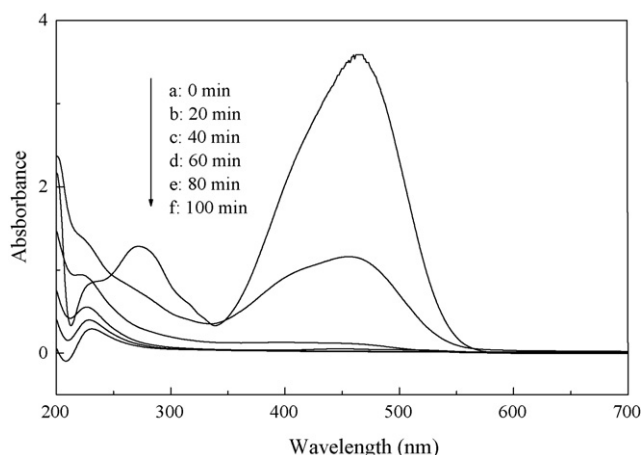


Fig. 3. UV-vis spectral changes of MO in heterogeneous UV-Fenton process. Experimental conditions: MO concentration = 50 mg l⁻¹, catalyst dose = 2.5 g l⁻¹, and H₂O₂ concentration = 15.8 mM, pH 7.0.

to 180 min, the MO in the low concentration of oxidant was also photodegraded fully.

We also studied the effect of initial pH in the range of 5.0–9.0 and the results are presented in Fig. 2(c). In this study, all the photodegradation processes were efficient and no evident differences were seen in the pH range of 5.0–9.0, which greatly differs from previous results. For example, Devi et al. [15] reported that the effect of pH on the photodegradation of MO in the system of zero valent iron powder/H₂O₂, the efficiency was halted in the pH range of 5.0–9.0, just like a homogeneous system. Hsueh et al. [16] also reported that the degradation rate of RB5 (Reactive Black 5) decreased sharply as the initial solution pH increased from 5.0 to 9.0. In addition, the removal ratios for our study after 120 min irradiation were above 99% within the pH range of 5.0–9.0. The reaction rate constants from 5.0 to 7.0 within 80 min were calculated by using a pseudo-first-order model and were 0.0489, 0.0549 and 0.0425 min⁻¹, respectively, namely, the rapid effect of photodegradation extended to a wider alkaline range and the removal of MO show no evident decreases with increasing pH. This observation was very important since it was previously accepted that one major drawback of the homogeneous photo-Fenton was the tight range of pH for its reaction.

The phenomenon that the UV-Fenton catalyst could extend the range of pH values for Fenton-type oxidation was also reported using iron-exchanged pillared beidellite [17] and iron-exchanged pillared bentonite [6] as the catalyst. This property should be ascribed to the acid-alkaline buffering capacities of the catalyst caused by Fe-polycations [Fe_n(OH)_m(H₂O)_x]^{(3n-m)+} [6], which were intermediate derivatives between the primary hydrolyzed products and the insoluble FeOOH. In the alkaline condition, most bases would be consumed by the Fe-polycations, and as a result, the degradation of MO could occur effectively by the UV-Fenton process just as in acidic conditions.

3.3. UV-vis spectroscopic analysis

Fig. 3 shows the time evolutions of the UV-vis spectra of MO during the decolorization process in the presence of the catalyst. The strong absorbance band at the visible region (at 460 nm) in MO was attributed to a conjugated structure formed by the azo bond under the strong influence of the electron-donating dimethylamino group, and the band at 270 nm was ascribed to the $\pi \rightarrow \pi^*$ transition related to aromatic rings [18]. After 20 min reaction, both bands at 465 and 270 nm became weaker, while absorbance at a lower UV region (near 200 nm) increased, due to the formation of

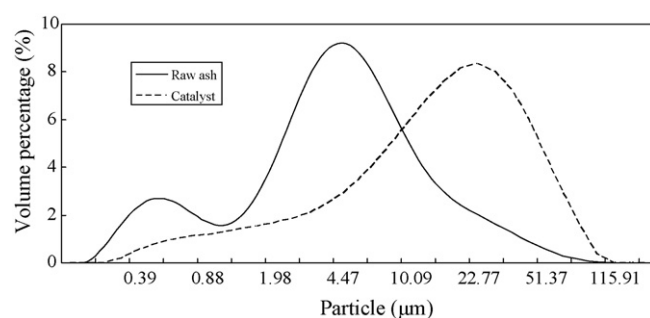


Fig. 4. Particle size distribution of the raw fly ash and the catalyst.

intermediate benzene-like organic compounds during the process of degradation [15]. Moreover, a new UV band at 226 nm became clear after 40 min, which should be ascribed to sulfanilic acid-like compounds [19].

After 60 min of irradiation, the solution was fully decolorized to transparency, and the corresponding absorbance at 460 nm completely disappeared in the spectrograph. Moreover, both the absorbance region near 200 nm and the peak at 226 nm also decreased, which indicates that when the intermediates of degradation in the solution accumulated to a certain concentration, the intermediates also began to degrade along with the degradation of the residual MO. In the remaining irradiation time, the absorbance region near 200 nm and the band at 226 nm continued decreasing until nearly completion, indicating that the MO and the intermediate species were completely degraded.

3.4. Separation of the catalyst from the solution

The separation of the catalyst from the solid into the liquid phase after the heterogeneous reaction is one of the important issues. Undoubtedly, the larger the powder size, the more efficient the catalyst is on the solid phase.

The particle size distributions of the raw ash and the catalyst are shown in Fig. 4, their particle size parameters and BET specific surface areas are shown in Table 1. According to the results, the raw ash distributed in the range from 0.295 to 116 μm and the catalyst was from 0.389 to 120 μm, correspondingly, their mean particle sizes were 5.51 and 21.1 μm respectively, which indicated that the catalyst had a much bigger size than the raw ash, and its median size was nearly 4 times larger than the raw ash, thus it can efficiently accelerate separation after the photo-Fenton reaction. In a contrast experiment, equivalent raw fly ash replaced the catalyst in the solution under the same conditions. The solution was turbid and it took more than 2 h for the solution to become clear, but it took only several minutes for the powder of catalyst to do that.

Generally speaking, increase of particle size can reduce its specific surface area due to increase of powder diameter, but in this study, specific surface area of the catalyst did not decrease, contrarily, it increased sharply. Table 1 shows that the BET surface area of the raw ash and the catalyst were 6.23 and 140 m²/g, respectively. Namely, loading amorphous FeOOH on the surface of acidized fly ash particles increased the specific surface area by nearly 22 times

Table 1
Particle size parameters and specific surface areas of the raw ash and the catalyst.

	$D(10)^a$, μm	Median size $D(50)$, μm	$D(90)^b$, μm	BET surface area, m ² /g
Raw ash	0.85	5.51	22.3	6.23
Catalyst	2.76	21.1	61.3	140

^a $D(10)$ means 10% of the powder particles are smaller than this value.

^b $D(90)$ means 90% of the powder particles are smaller than this value.

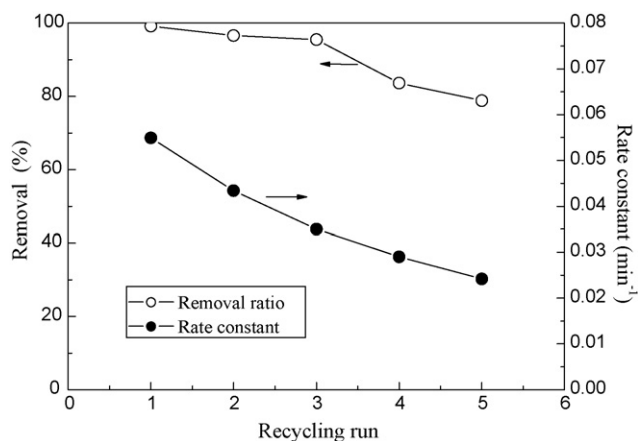


Fig. 5. Removal ratio and rate constant of five recycling runs. Experimental conditions: MO concentration = 50 mg l⁻¹, catalyst dose = 2.5 g l⁻¹, H₂O₂ concentration = 15.8 mM, time = 80 min, and pH 7.0.

compared to the raw ash, which could be attributed to the formation of mesoporous amorphous FeOOH. Thus it can enhance the adsorption of the catalyst and increase the interface between MO and the catalyst, thus more active surface sites of Fe(OH)²⁺ supported on the surface of fly ash are prone to contact with MO molecules and thus accelerate the photo-Fenton process.

3.5. Recycling efficiency of the catalyst

The recycling efficiency of the photo-Fenton reagent was tested by recycling the catalyst for decolorizing the MO dye. Experiments were carried out for 80 min at pH of 7.0 and H₂O₂ concentration of 26.3 mM. After each run, the solid powder was carefully separated from the solution, and then rinsed by 50 ml of water and non-aqueous ether for 3 times respectively, for removing any possible remnants on the surface of catalyst. Then, fresh MO solution along with the H₂O₂ oxidant was placed in the reactor using the same catalyst powder. For the first three runs of the experiment, all MO decolorizations were above 95% (99.2, 96.6, 95.5% in turn), followed by a small decrease, although the rate constant of decolorization decreased steadily throughout (0.0549, 0.0434, 0.0356 min⁻¹) (Fig. 5). On the fourth and fifth runs the efficiency of the catalyst decreased to 83% and 78%, respectively, with the corresponding rate constants decreasing to 0.0295 and 0.0252 min⁻¹, which could be attributed to an unavoidable leaching of iron and possible effect of contaminant adsorption on reactive sites on the catalyst surface. Nevertheless, when the reaction time prolonged to 120 min, all MO decolorization ended up above 99%.

3.6. Stability of amorphous FeOOH

Pure amorphous FeOOH is unstable as it tends to crystallize under mild conditions, with consequent decrease in the specific surface area. Therefore, the degree of stability of the amorphous FeOOH supported on the surface of fly ash is an important property of the catalyst. For testing the stabilization of catalyst, the aging time in the synthesis was extended from 3 to 7 days and the final solution pH was adjusted from 3.0 to 12.0 to promote any possible nucleation of iron hydroxides/oxides, but all XRD patterns of the obtained powders showed no variation in contrast with that at the aging time of 3 days and pH 6.0 (XRD patterns were not shown here.). It showed that amorphous FeOOH in the catalyst was stable and no crystalline iron oxides were formed. But when pure chemical reagents were used as the raw materials in the similar hydrothermal conditions, iron hydroxides/oxides were formed. For

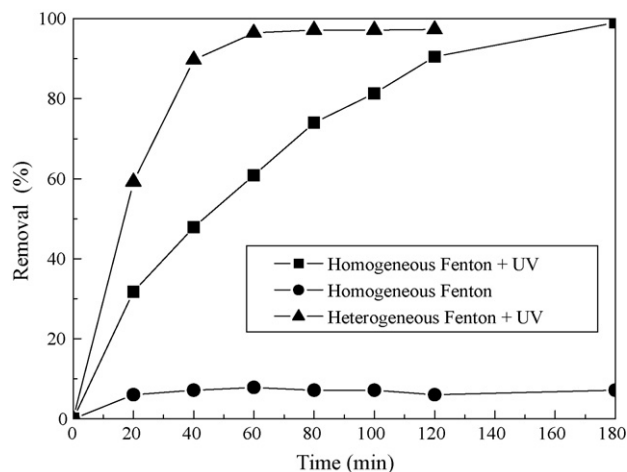


Fig. 6. Effect of homogeneous and heterogeneous catalysis on the degradation of MO. Experimental conditions for the heterogeneous Fenton: MO concentration = 50 mg l⁻¹, catalyst dose = 2.5 g l⁻¹, H₂O₂ concentration = 15.8 mM, pH 7.0; for the homogeneous Fenton: MO concentration = 50 mg l⁻¹, [Fe³⁺] = 0.46 g l⁻¹, H₂O₂ concentration = 15.8 mM, and pH 7.0.

example, Zhang and Ma [20] reported α -FeOOH (goethite) formed in the similar reaction scopes. The stability of amorphous FeOOH supported on the acidized fly ash can be attributed to the reasons discussed below.

During the process of preparation, the fly ash contacted with the acidic solution firstly, and Si–O bond on the surface of the spherical glassy particles increased due to dissolution of the metal elements. Afterwards, when FeOOH precipitated from the aqueous solution and coated on the surface of the residual fly ash, Fe–Si surface complex (typically, Fe–O–Si(OH)₃) formed in situ as reported in the previous literatures [21,22], hence blocked or retarded the transformation of initially formed FeOOH to crystalline iron oxides such as ferrihydrite, goethite and hematite.

3.7. Influence of the homogeneous Fenton

Undoubtedly, the leached iron is generated at lower pH (below 4.0) due to the reductive dissolution of FeOOH [4] and consequently, it can assist the Fenton reaction even in the heterogeneous system. Besides pH, the concentration of leaching iron varies by the irradiation time, concentration of H₂O₂ and catalyst dosage [23].

To understand whether dissolved iron from the catalyst would contribute significantly to the decomposition of MO, the dissolved iron concentration was measured in one of the heterogeneous Fenton experiments. In the presence of 2.5 g l⁻¹ catalyst (theoretically 0.46 g Fe l⁻¹) and 15.8 mM H₂O₂ at initial pH 7.0, the photocatalytic decomposition rate of MO was nearly 99% after 60 min reaction (Fig. 6) and the highest leaking iron concentration within 120 min measured was 0.26 mg l⁻¹, which was quite below the max leaking value of 0.95 mg l⁻¹ reported for α -FeOOH Fenton system with the similar iron dosage (5 g l⁻¹ α -FeOOH and theoretically 0.5 g Fe³⁺ l⁻¹) and the initial reaction pH (7.47) [23]. This was mainly ascribed to the following two reasons. One was that the leached iron species may quickly hydrolyze and age relative quickly to more stable (less soluble) particulate iron oxyhydroxides forms at pH 7.0. Another was that the amorphous FeOOH supported on acidized fly ash was intrinsically stable (above mentioned) and not easy to dissolve into the solution, thus the dissolved iron concentration was very low in this system. Moreover, the leaching iron concentration was well below the EU directives, which allow a maximum of 2 mg l⁻¹ in the treated water to be discharged directly into the environment.

The control homogeneous Fenton experiments (using $0.26 \text{ mg Fe}^{3+} \text{ l}^{-1}$ as Fenton reagent) were arranged with and without UV light. The results are shown in Fig. 6. The traditional homogeneous Fenton without UV irradiation, the removal of MO of 20 min attained 6%, and as the irradiation time extended to 180 min, no evident change of the removal was observed and the removal kept stable unlike the fluctuation of removal of MO in heterogeneous Fenton which was due to adsorption (Fig. 2(a)).

When UV irradiation was used, the catalytic performance of the homogeneous Fenton enhanced, nevertheless, it was less than that of heterogeneous photo-Fenton process. The removal of MO at this level of dissolved iron concentration was about 60.8% after 60 min reaction while that of heterogeneous photo-Fenton process was 96.4%. Until the irradiation time extended to 180 min, the removal of the homogeneous Fenton system with UV irradiation can also attain 97.8%, indicating that the irradiation time of the heterogeneous Fenton was nearly 120 min less than that of the homogeneous Fenton when MO was completely decolorized.

4. Conclusions

Through dissolution and precipitation processes using a high iron-containing fly ash as the raw material, amorphous FeOOH was successfully loaded on the surface of residual ash after acidized, and used as the catalyst in UV-Fenton system for the degradation of MO. The mesoporous structure of FeOOH provided a wide contact interface between the catalyst and the MO molecules, and accelerated the heterogeneous Fenton process. The catalyst exhibited a high catalytic activity and almost 100% discoloration of 50 mg l^{-1} MO could be obtained at 80 min reaction even if the initial pH of solution was as high as 9.0, so the catalyst enabled operation at around the neutral and alkaline solution. Moreover the catalyst was of great importance for application due to its good stability, easy physical solid–liquor separation, little iron leaching and no need to be regenerated.

Acknowledgements

This work was financially supported by the National Key Technology R&D Program (2008BAC32B03), the National Basic Research Program (2007CB407303) and the National Water Pollution Control Program (2008ZX07012-002-004) of China.

References

- [1] F.J. Rivas, F.J. Beltrán, J. Frades, P. Buxeda, Oxidation of *p*-hydroxybenzoic acid by Fenton's reagent, *Water Res.* 35 (2001) 387.

- [2] J. He, W. Ma, J. He, J. Zhao, J.C. Yu, Photooxidation of azo dye in aqueous dispersions of $\text{H}_2\text{O}_2/\alpha\text{-FeOOH}$, *Appl. Catal. B: Environ.* 39 (2002) 211.
- [3] J.J. Wu, M. Muruganandham, J.S. Yang, S.S. Lin, Oxidation of DMSO on goethite catalyst in the presence of H_2O_2 at neutral pH, *Catal. Commun.* 7 (2006) 901.
- [4] S. Chou, C. Huang, Y.-H. Huang, Heterogeneous and homogeneous catalytic oxidation by supported $\gamma\text{-FeOOH}$ in a fluidized-bed reactor: kinetic approach, *Environ. Sci. Technol.* 35 (6) (2001) 1247.
- [5] X. Wang, C. Liu, X. Li, F. Li, S. Zhou, Photodegradation of 2-mercaptobenzothiazole in the $\gamma\text{-Fe}_2\text{O}_3/\text{oxalate}$ suspension under UVA light irradiation, *J. Hazard. Mater.* 153 (2008) 426.
- [6] J. Chen, L. Zhu, UV-Fenton discoloration and mineralization of orange II over hydroxyl-Fe-pillared bentonite, *J. Photochem. Photobiol. A: Chem.* 188 (2007) 56.
- [7] B. Iurascu, I. Siminiceanu, D. Vione, M.A. Vicente, A. Gil, Phenol degradation in water through a heterogeneous photo-Fenton process catalyzed by Fe-treated laponite, *Water Res.* 43 (2009) 1313.
- [8] C.-L. Hsueh, Y.-W. Lu, C.-C. Hung, Y.-H. Huang, C.-Y. Chen, Adsorption kinetic, thermodynamic and desorption studies of C.I. Reactive Black 5 on a novel photoassisted Fenton catalyst, *Dyes Pigments* 75 (2007) 130.
- [9] J.H. Ramirez, F.J. Maldonado-Hódar, A.F. Pérez-Cadenas, C. Moreno-Castilla, C.A. Costa, L.M. Madeira, Azo-dye Orange II degradation by heterogeneous Fenton-like reaction using carbon-Fe catalysts, *Appl. Catal. B: Environ.* 75 (2007) 312.
- [10] B. Muthukumari, K. Selvam, I. Muthuvel, M. Swaminathan, Photoassisted hetero-Fenton mineralisation of azo dyes by Fe (II)- Al_2O_3 catalyst, *Chem. Eng. J.* 153 (2009) 9.
- [11] J.R. Domínguez, J. Beltrán, O. Rodríguez, Vis and UV photocatalytic detoxification methods (using TiO_2 , $\text{TiO}_2/\text{H}_2\text{O}_2$, TiO_2/O_3 , $\text{TiO}_2/\text{S}_2\text{O}_8^{2-}$, O_3 , H_2O_2 , $\text{S}_2\text{O}_8^{2-}$, $\text{Fe}^{3+}/\text{H}_2\text{O}_2$ and $\text{Fe}^{3+}/\text{H}_2\text{O}_2/\text{C}_2\text{O}_4^{2-}$) for dyes treatment, *Catal. Today* 101 (2005) 389.
- [12] Y. Li, F.-S. Zhang, R.-X. Fu, Arsenic (V) removal from aqueous system using adsorbent developed from a high iron-containing fly ash, *Sci. Total Environ.* 407 (2009) 5780.
- [13] M.J. Liou, M.-C. Lu, Catalytic degradation of explosives with goethite and hydrogen peroxide, *J. Hazard. Mater.* 151 (2008) 540.
- [14] V. Kavitha, K. Palanivelu, The role of ferrous ion in Fenton and photo-Fenton processes for the degradation of phenol, *Chemosphere* 55 (2004) 1235.
- [15] L.G. Devi, S.G. Kumar, K.M. Reddy, C. Munikrishnappa, Photo degradation of Methyl Orange an azo dye by advanced Fenton process using zero valent metallic iron: influence of various reaction parameters and its degradation mechanism, *J. Hazard. Mater.* 164 (2009) 459.
- [16] C.-L. Hsueh, Y.-H. Huang, C.-C. Wang, C.-Y. Chen, Photoassisted fenton degradation of nonbiodegradable azo-dye (Reactive Black 5) over a novel supported iron oxide catalyst at neutral pH, *J. Mol. Catal. A: Chem.* 245 (2006) 78.
- [17] C. Catrinescu, C. Teodosiu, M. Macoveanu, J. Miehle-Brendle, R.L. Dred, Catalytic wet peroxide oxidation of phenol over Fe-exchanged pillared beidellite, *Water Res.* 37 (2003) 1154.
- [18] C. Galindo, P. Jacques, A. Kalt, Photodegradation of the aminoazobenzene acid orange 52 by three advanced oxidation processes: UV/ H_2O_2 , UV/ TiO_2 and VIS/ TiO_2 : comparative mechanistic and kinetic investigations, *J. Photochem. Photobiol. A: Chem.* 130 (2000) 35.
- [19] J. Fan, Y. Guo, J. Wang, M. Fan, Rapid decolorization of azo dye Methyl Orange in aqueous solution by nanoscale zerovalent iron particles, *J. Hazard. Mater.* 166 (2009) 904.
- [20] T. Zhang, J. Ma, Catalytic ozonation of trace nitrobenzene in water with synthetic goethite, *J. Mol. Catal. A: Chem.* 279 (2008) 82.
- [21] P.J. Swedlund, J.G. Webster, Adsorption and polymerisation of silicic acid on ferrihydrite and its effect on arsenic adsorption, *Water Res.* 33 (1999) 3413.
- [22] F.-S. Zhang, H. Itoh, Iron oxide-loaded slag for arsenic removal from aqueous system, *Chemosphere* 60 (2005) 319.
- [23] Y. Zhao, J. Hu, Photo-Fenton degradation of 17 β -estradiol in presence of $\alpha\text{-FeOOH}$ and H_2O_2 , *Appl. Catal. B: Environ.* 78 (2008) 250.